EISCAT SPACE DEBRIS DURING THE IPY — A 5000 HOUR CAMPAIGN

J. Markkanen[1], R. Jehn[2], and H. Krag[2]

[1]*EISCAT, Tähteläntie 56, 99600 Sodankylä, Finland, Email: jussi.markkanen@sgo.fi*
[2]*ESA/ESOC, Robert-Bosch-Str. 5, 64293 Darmstadt, Germany*

ABSTRACT

During the International Polar Year (IPY) in 2007-2009, EISCAT measured space debris at its Svalbard radar (ESR, latitude 78.2°N), simultaneously with the standard ionospheric measurement. From the 239 000 events which were recorded in 5060 hours only a "Quality Set" (QS) was extracted for further analysis. The QS essentially consists of 101 complete 24-hour beam park debris measurements, between 13 Mar 2007 and 10 Feb 2008, and contains about 95 000 events. The data provide a relatively dense sampling of the debris environment above ESR in the first year following the Chinese ASAT event, in January 2007. The QS is freely available in the web.

Key words: EISCAT; Space debris; International polar year; ASAT.

1. INTRODUCTION

For the two-year long international polar year, from March 2007 to March 2009, EISCAT Svalbard Radar (ESR), attempted to increase its operation from around the normal 2000 hours a year to an essentially continuous coverage, with the aim of producing the most detailed and extensive record of the high latitude ionosphere ever recorded.

During three ESA contracts between 2000 and 2005, EISCAT had constructed a space debris receiver for ESR, separate from the receivers used in ionospheric work, and developed the necessary data processing, so that debris measurements could be performed in parallel with the ionospheric measurements, using common transmission but different data processing [1]-[4]. In February 2007 the space debris receiver, though unused for some time, was still in good shape and it was decided at the last minute to attempt a series of debris observations as well, as a low priority, minimum cost project. For the whole IPY campaign, the space debris receiver was operated over the internet from EISCAT Sodankylä site in Finland.

EISCAT started the ionospheric IPY operation on 1 March 2007, but it took a few days to bring the debris receiver and the software out of hibernation and to configure them for the IPY measurement. The first full 24-hour day with the debris receiver was recorded on 13 March. When the data were analysed using EISCAT's standard procedure, which is summarized in section 2, and the hourly event count plotted, the plot, similar to Fig. 4a, came out as a big surprise. There had never been a single fragmentation event evident in EISCAT debris data earlier, and the news about the 11 January 2007 Chinese ASAT event had not yet reached EISCAT. The two big daily increases in the hourly event count, one at around 06 UT and the other around 12 UT, were finally identified as the signature of the Earth-fixed ESR radar beam crossing the ASAT debris ring twice a day.

Once it was understood that it would be possible to follow the aftermath of a major fragmentation event during the IPY campaign, it was decided to try to improve the standard debris data processing to get better altitude coverage. Originally, the altitude coverage was between 225 km and 2090 km in four 190 km wide zones (see e.g. Fig. 5a). By handling also situations where part of the target echo is masked by a transmission window the altitude coverage was increased by 77%. The new, wider altitude zones are: zone 1 149–489 km; zone 2 706–1047 km; zone 3 1264–1605 km; and zone 4 1823–2164 km (Fig. 5b). Even the wider zones cover only about two thirds of the LEO altitude. Besides losing the targets in the gaps, the gaps, and the gap edges, cause considerable problems in the analysis. Luckily, in an otherwise unfortunate affair, the ASAT event had occurred near the centre of the zone 2, and was therefore well visible at ESR. It took considerable time to modify the data processing, and it was only from 5 May onwards that the wider zones could be exploited.

Early in the campaign it also became evident that the data processing infrastructure that had been developed in the ESA contracts, to be able to routinely handle large-scale data processing, was not quite up to the task. In practice, considerable daily manual work was still needed, and the task was quickly becoming unmanageable. The problem was solved by writing a set of Matlab and Unix shell scripts that were able to handle the whole data processing chain, from signal sampling to the publishing of analysis results in the web, entirely without operator intervention.

Automated debris data processing was finally in place in late spring, and for the rest of the IPY campaign, only an occasional check was needed. Unsurprisingly for such a long campaign, there were some problems at the ESR site, including a fire that destroyed a transmitter transformer unit, and an almost one-month data gap in the autumn 2007 when the whole site was without sufficient power due to problems at the Svalbard electric power station.

Late in 2007 it become evident that EISCAT's original plan to measure continuously throughout the two-year IPY period was not going to succeed. The burden for the understaffed ESR site working under the harsh polar conditions was just too large; and due to the large amount of staff overtime, funding was also becoming an issue. It was decided to scale down the radar operation for the second IPY year. From March 2008 to March 2009, ESR performed an 30 hour IPY measurement once every two weeks only. Almost all of those measurements were in "ipy2" mode that uses a three-position antenna scan. During the first IPY year, the principal mode had been "ipy1", which uses a fixed, magnetic-field-aligned pointing, though ipy2 had also been used occasionally. Moreover, starting already from the beginning of 2008, the normal practice of EISCAT user groups performing their own measurement campaigns at ESR, which had been suppressed during the first IPY year, was re-introduced.

The automated IPY debris operation had been hard-coded for the ipy1 mode. As the special measurements started to cause increasing number of gaps in the debris data records, the debris campaign was finally given up late in February 2008. The last complete 24-hour period is from 10 February 2008.

From the 335 day period from 13 March 2007 to 10 February 2008, the initial analysis produced 239 000 unique beam-passage events. From the 8040 hour interval, debris measurement was active for 5060 hours. The latter number is computed from the analysed data, by summing up all 30-minute intervals from which there is at least one successfully analysed event.

A significant part of the 239 000 primary events are problematic, or at least in need of special attention. Rather than attempting manual correction case-by-case, it was decided to perform some form of further selection that could be applied automatically, and could be expected to get rid of most of the problem data. When all weak (below a certain threshold signal strength) and very-short-duration events, and also all the days during which the antenna was not operating in the ipy1 mode the whole day, are removed, one is left with a set of 101 quality days, with about 95 000 events. This "quality set" (QS) is the final analysis result of the IPY debris campaign.

The QS is in the public domain, and can be accessed via the EISCAT IPY debris web page at `www.sgo.fi/~jussi/spade/ipy/index.html`. Three days of the QS were used in 2007 to compare the event counts predicted by ESA's PROOF tool to the EISCAT measurements, in order to estimate the number of small-size particles in the ASAT cloud [5], [6].

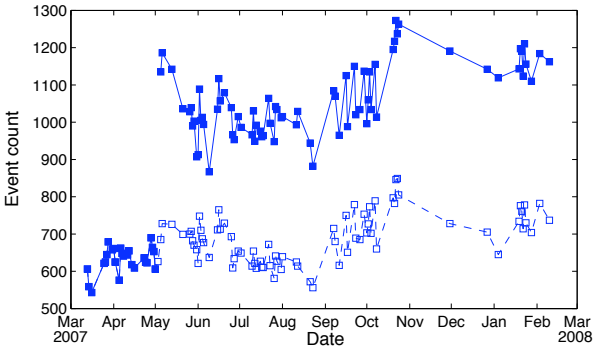

Figure 1. Daily debris event count during the IPY. The solid dots are the actual event counts from all the 101 days in the Quality Set. The open dots give the event count as restricted to the initial, narrower, altitude zones that were in use until 4 May 2007.

Figure 1 shows the daily event count in the QS. Except for the late autumn 2007, the QS provides a reasonably dense sampling of the first IPY year. This makes it possible to inspect both day-to-day variations, as well as longer-term trends, of the ASAT cloud, and compare to the predictions of debris models. After an overview of EISCAT debris measurement and analysis scheme in the next section, in the final section we first give a few examples of the daily data, then use PROOF to explain a curious periodic variation in the observed daily debris event density during the IPY.

2. DETECTION AND PARAMETER ESTIMATION

The IPY debris data were recorded with the EISCAT space debris receiver, attached to the Svalbard 32 m dish (the site is at $78.2°\mathrm{N}, 16.0°\mathrm{E}$), which has power gain G_{rx} of 42.5 dBi. The transmission was via the other of the two ESR antennas, the 42 m dish, which is located a few tens of meters from the 32m antenna, and has power gain G_{tx} of 45.3 dBi. Both antennas were pointed to elevation $81.6°$ and azimuth $182.1°$. This bi-static arrangement was actually an accident, due to a wrongly connected cable. When the unintended configuration was noticed late in the spring 2007, it was deemed better to keep the connection as it was, rather than to change an important parameter in the middle of the campaign.

The EISCAT IPY experiment (both the ipy1 and ipy2 modes) uses a set of 64 different 30×30 μs phase-coded pulses for transmission. The 900 μs pulses are sent using an interpulse period of 3750 μs, and the 0.24 s cycle then repeats. During the campaign the transmission peak power varied, often in rather sharp steps, between 0.5 MW and 0.9 MW, depending on how many transmitter modules had been tripped at the time (see Fig. 4).

Nevertheless, a constant daily transmission peak power near 0.8 MW was used in the analysis. The actual transmission power value is stored in files, so re-analysis in this respect would be possible. But this would only affect the RCS estimates, which are quite uncertain anyway. Transmission frequency was 499.85 MHz.

A constant receiver noise temperature $T_{\rm noise}$ of 75 K was assumed in the analysis, while the true noise temperature at ESR typically varies daily between about 60 K and 90 K (Fig. 4) due to sky noise variation. The digitally implemented space debris receiver always has noise-equivalent bandwidth $B_{\rm eq}$ matched to the sampling rate; during the IPY, $B_{\rm eq}$=200 kHz. The EISCAT space debris receiver, sampling continuously also during transmission, produced 16+16 bit complex-valued base-band samples with final sampling interval of 5.0 μs. The samples were written to disk with the rate of 2.7 GBytes/hour, and stored for a few days.

Debris detection and parameter estimation is based on coherent integration, implemented through the evaluation of what we prefer calling the "match function" (MF), but which more commonly is known as the radar ambiguity function. An example is shown in Fig. 2. The MF is a measure of how closely a two-parameter (range R and radial Doppler-velocity v) model $\chi(v, R; t)$ of the received signal resembles the actually measured signal. When computing the MF for a time interval $[t_0, t_0 + T_{\rm c}]$, where $T_{\rm c}$ is the length of the coherent integration, a received data segment $z(t)$ of duration $T_{\rm c}$ is compared against the model functions in the inner-product (cross correlation) sense

$$\mathrm{MF}(v, R) = \frac{|\langle \chi(R, v), z \rangle|}{\|\chi\|} \,. \qquad (1)$$

During the IPY campaign, we used $T_{\rm c}$=0.24 s. The MF maximum position in the v, R plane gives an estimate of the range and the Doppler-velocity during the integration. For a phase-coherent noiseless signal, the MF achieves coherent integration of the samples, in the sense that the maximum value of the MF equals the sum of the amplitudes of the complex samples (up to a normalization). We normalize the MF so that the value of the MF maximum gives an estimate of the ratio ENR of the total signal energy $E_{\rm sig}$ to the noise power spectral density $k_{\rm B}T_{\rm noise}$, $\mathrm{ENR} \equiv E_{\rm sig}/k_{\rm B}T_{\rm noise}$. The estimate is

$$\mathrm{ENR} \sim \frac{\max_{v,R} \mathrm{MF}^2}{\sigma^2_{\rm noise}} \,, \qquad (2)$$

where $\sigma^2_{\rm noise}$ is an estimate of the noise variance. Detection criterion is the ENR exceeding a range-dependent threshold value. The threshold was kept fixed for the whole IPY campaign duration. Once the ENR is found, an estimate of the radar cross section (RCS) of the target can be found via the standard radar equation, which for the bi-static, but now essentially backscatter, case can be written as

$$\mathrm{ENR} = \frac{E_{\rm tx}}{k_{\rm B}T_{\rm noise}} \cdot \frac{G_{\rm tx}(\theta)}{4\pi R^2} \cdot \frac{\mathrm{RCS}}{4\pi R^2} \cdot \frac{G_{\rm rx}(\theta)\lambda^2}{4\pi} \,. \qquad (3)$$

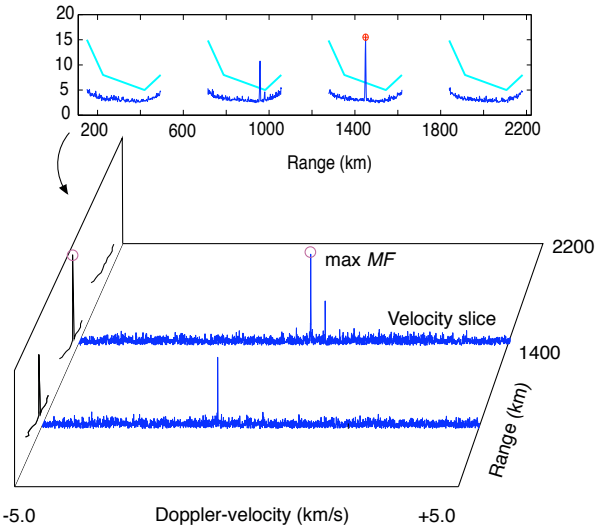

Figure 2. Match function as used in the IPY detections. The quantity plotted in the bottom panel is $\mathrm{MF}(v, R)/\sigma$*, but only two out of the total of about 1000 velocity slices are actually drawn. For detection, the two-parameter* MF *is computed and maximized per each 0.24 s coherent integration. In the top panel, and schematically at the left in the bottom panel, is plotted the function* $R \mapsto \max_v \mathrm{MF}(v, R)/\sigma$*. The function is a convenient one-dimensional quantity to indicate the ranges of the targets. In this case, there are two targets in the beam exceeding the range-dependent detection threshold. The threshold is shown by the light-blue line in the top panel.*

Here $E_{\rm tx}$ is the total transmission energy during the coherent integration, computed from the assumed peak power of 0.8 MW, and the number 64 of the 3750 μs pulses used in the coherent integration. (The energy is 190 kJ in this case.) In the EISCAT case, the offset angle θ of the target from the beam optical axis is not known. What is given in the result listings is a minimum value of RCS, solved from the equation by assuming the target is at the centre of the beam.

The match function $\mathrm{MF}(v, R)$ for the IPY scheme is shown schematically in Fig. 2. The figure also shows the actual detection threshold used during the IPY campaign, and shows the four altitude zones and the altitude gaps. Essentially by trial end error, in the early phase of the campaign, the detection threshold was set so high that only a "modest amount" of false detections will occur even in the worst conditions. The problem is the variable, and often strong, ionospheric clutter, which in Fig. 2 is responsible for the increase in the MF level towards the smaller ranges, in all altitude zones. The increase towards the higher ranges instead is due to the receiver calibration noise that EISCAT injects to the receiver every now and then, as well as to the special handling needed for the increased range coverage. In the example, showing typical situation in mid winter, the clutter is not particularly strong, and the detection threshold is unnecessarily conservative. However, this changes during summer, and also in winter during auroral events. For the IPY QS,

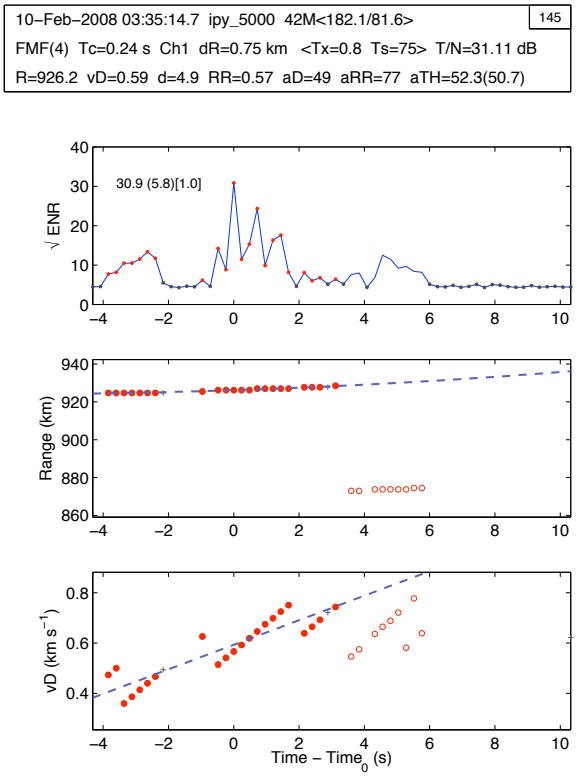

Figure 3. An event summary plot from the last day of the IPY campaign. A similar plot is available for each event of the campaign. The data points are also available in numerical form. The header panel gives the time t_0 of the maximum ENR*, some experiment set-up info, and the main analysis result parameters. These are the range $R(t_0)$ in km from quadratic fit to the $R(t)$ data; Doppler-velocity $v_{\rm D}(t_0)$ in $\mathrm{km\,s^{-1}}$ from linear fit to the $v_{\rm D}(t)$ data; effective diameter d in cm; range rate* $\mathrm{RR}(t_0)$ *from the $R(t)$ data; Dopper-drift (time derivative of $v_{\rm D}$) $a_{\rm D}(t_0)$ in $\mathrm{m\,s^{-2}}$ from the $v_{\rm D}(t)$ data; Doppler-drift $a_{\rm RR}(t_0)$ from $R(t)$ data; and, for comparison, the Doppler-drift $a_{\rm TH}$ expected for a target in a circular polar orbit through the range $R(t_0)$. The solid circles are used for the fits, the open circles represent another target, at about 880 km altitude, which is disregarded here. In the $v_{\rm D}(t)$ panel, the odd-looking slope and the discontinuities are artifacts due to the "fast" version of the match function that was used in the analysis computations (see e.g. [2], pp. 40-53).*

a range-independent selection threshold ENR=100 was imposed after analysis, in an effort so somehow simulate a flat detection threshold. The result is that the target size (and RCS) distributions are distorted, as if artificially cut towards the smaller sizes. This should be kept in mind when comparing the data with models. In retrospect, it might have been better if one had used such an exceptionally high but flat threshold already in the detection phase.

During the IPY, the detections were done in (almost) real-time, and information saved to files. Then, once per day, analysis was run, also locally at the ESR site. The analysis is performed in the following way: First, the set of detections is cleaned by using various heuristic algorithms to remove spurious detections due to targets that in reality are in the range gaps, or entirely outside of the monitored LEO range. These ghost targets are a nuisance in the high-duty-cycle, phase-coded EISCAT debris measurements. Range aliases from higher, unmonitored ranges can probably never be completely eliminated, but in the future, we hope to get rid of the gaps within LEO by using new transmission schemes that use variable-length interpulse periods [7].

In the next phase of the analysis, detections are grouped to beam-passage events. The raw data for each event are then copied separately to event-specific files. After that, the event parameters are estimated using the MF-method. Basically, the events' data are re-detected, now with maximal time and range resolution but only over a narrow range interval around the original detection range. For each event, the detections generate time series of ENR, range, and Doppler-velocity during the beam passage, as shown in the event summary plot in Fig. 3. The $R(t)$ and $v(t)$ points are fitted with linear or quadratic polynomials to find the range and Doppler for the time t_0 of maximum value of $\mathrm{ENR}(t)$. These parameters, together with some others like the RCS and the effective target diameter d derived from it, and some estimates for the rate of change of the Doppler-velocity as mentioned in the caption of Fig. 3, are saved to daily result listings.

Inspection of an event summary plot often reveals more than one target in the data, like the target at around 880 km range in Fig. 3. Sometimes these weaker (but still quite strong) targets can be found somewhere else in the final result listings, but often, like in the case of Fig. 3, they are entirely missed by the automatic analysis. This must be considered a flaw in the analysis procedure, and should not be too difficult to remedy in the future. If one compares the EISCAT events to debris catalogues, one should keep in mind that even some strong expected events can be missing from the QS if there are even stronger events nearby in time.

Besides the result listings and the event summary plots, also the detection scans were saved in the daily analysis result files, so that if one wants afterwards to inspects in detail some particular event, there are some possibilities for that. However, due to lack of disk space, it was not possible to save the original IPY raw signal samples permanently, and so the data cannot any more be re-analysed for longer integration, for better threshold in some particularly interesting altitude region, for better altitude coverage, nor anything else.

The daily analysis at ESR took about six hours on a 2 GHz Mac G5 workstation. The analysis result files were copied automatically, once per day, over internet to a workstation at Sodankylä EISCAT site. The workstation automatically produced daily data summary plots as six-page LaTeX-formated PDF documents, and copied the documents to the EISCAT IPY space debris web page.

That page contains also the weekly summary plots which were generated by a script that was run manually every now and then.

3. DATA

Table 1 lists the 101 days of the IPY Quality Set. This section gives some examples of that data.

Figure 4 shows half-hourly event count from the first and the last day of the campaign. Figure 4a gives the situation about two months after the ASAT event, when the debris ring is still quite narrow over ESR. The debris ring crossings are at about 06 UT and 12 UT. The ASAT cloud is much more spread eleven months later, in Fig. 4b.

When the ASAT debris ring was still narrow, the event count increase was much sharper at the noon crossing than at the morning crossing. This seems not be just a binning effect in the histogram, but the events actually seems to be more spread in time near 06 UT than at noon. This is rather evident in Fig. 5a, which shows the time-altitude distribution of the events (and, in addition, uses color-coding for the Doppler-velocity) at the beginning of the campaign. The observations clearly are more spread in time near 06 UT. Inspection of other early days shows considerable day-to-day variation, but the asymmetry is a persistent feature. It probably is due to an asymmetric ring-crossing geometry.

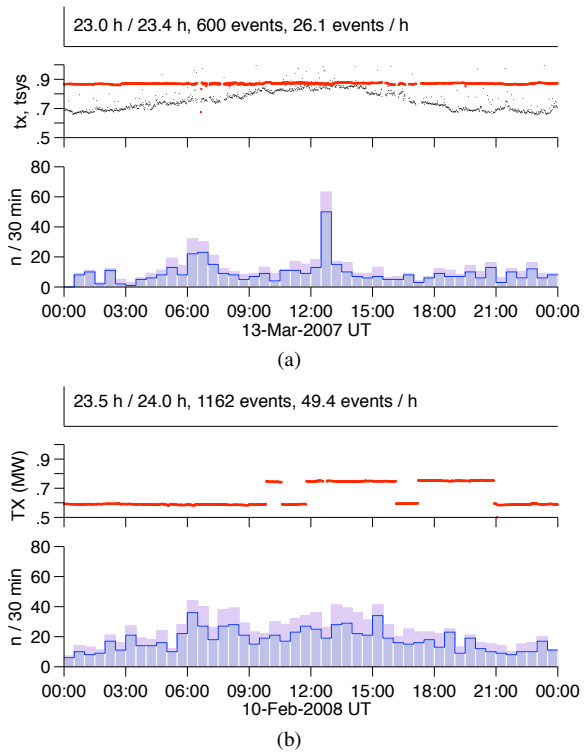

Figure 4. Half-hourly event count at the beginning (a) and end (b) of the IPY campaign. The red curves show the transmission power in MW. In (a), the gray curve is the noise temperature in units of 100 K. The light-colored histogram is the hourly count for all ($\sqrt{\mathrm{ENR}} > 10$), the histogram under the solid line restricts the count to the stronger events, with $\sqrt{\mathrm{ENR}} > 20$. Note that in (b), the experiment has about 77% larger altitude coverage than in (a).

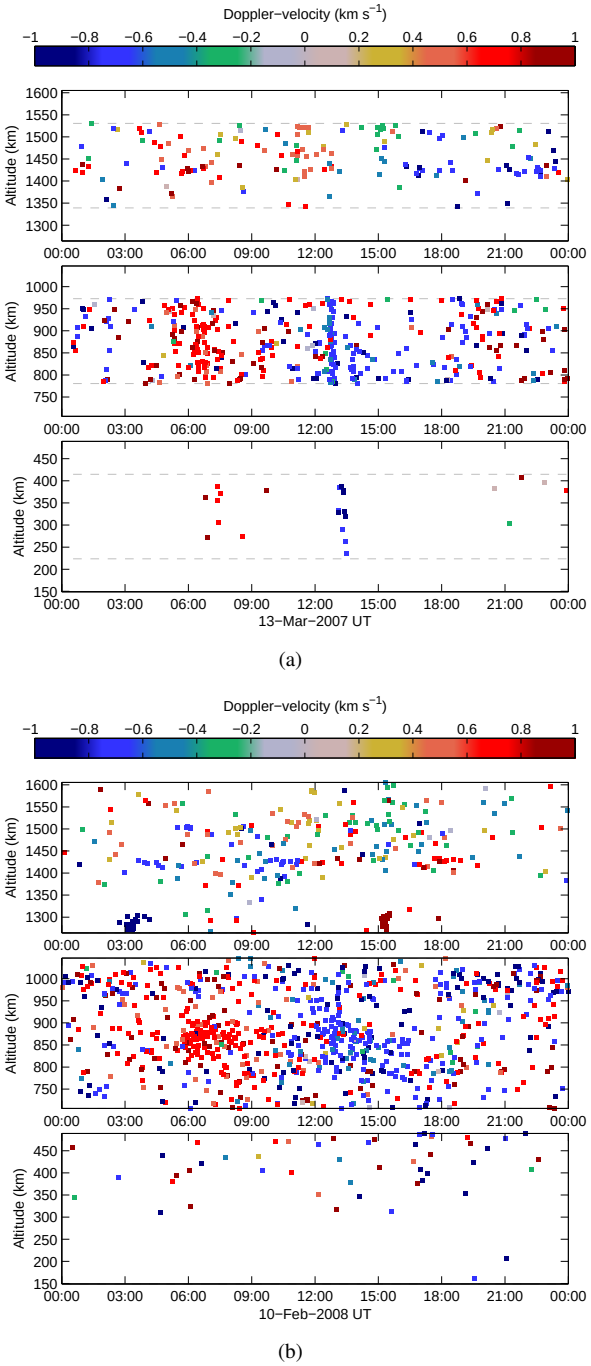

Figure 5. Time-altitude distribution of events in the three lowest altitude zones, at the beginning (a) and end (b) of the IPY campaign.

Table 1. The 101 dates of the Quality Set. Except possibly near midnight, these days have nearly uninterrupted data record from 0 UT to 24 UT. Both the IPY day number, counted from the beginning of the IPY on 1 March 2007, and the date label as YYMMDD are given.

13	070313	64	070503	133	070711	215	071001
14	070314	66	070505	134	070712	216	071002
16	070316	67	070506	135	070713	217	071003
25	070325	74	070513	138	070716	218	071004
26	070326	82	070521	139	070717	221	071007
27	070327	87	070526	140	070718	222	071008
28	070328	88	070527	144	070722	234	071020
31	070331	89	070528	145	070723	235	071021
32	070401	90	070529	148	070726	236	071022
33	070402	92	070531	149	070727	237	071023
36	070405	93	070601	150	070728	238	071024
37	070406	94	070602	153	070731	275	071130
38	070407	95	070603	154	070801	302	071227
39	070408	96	070604	164	070811	310	080104
40	070409	97	070605	165	070812	325	080119
42	070411	101	070609	174	070821	326	080120
43	070412	107	070615	176	070823	327	080121
45	070414	108	070616	191	070907	328	080122
47	070416	109	070617	192	070908	329	080123
54	070423	112	070620	195	070911	330	080124
55	070424	117	070625	200	070916	334	080128
56	070425	118	070626	201	070917	340	080203
59	070428	119	070627	206	070922	347	080210
60	070429	122	070630	207	070923		
61	070430	124	070702	210	070926		
62	070501	132	070710	213	070929		

Though the ASAT cloud is the most prominent feature in plots like Fig. 5, there is considerably structure also elsewhere. A conspicuous feature throughout the IPY (as soon as the altitude zones were expanded) were the two clusters seen in Fig. 5b near 03 UT and 15 UT at an altitude of about 1300 km. They drift in time from day to day, so they do not represent a sun-synchronous ring as the ASAT; rather, their Doppler-velocity is such that they could be on a near-90° inclination orbit. Their altitude also varies somewhat, but the altitude gap makes it impossible to monitor that variation properly. This is one of the places where it would be nice to be able to re-analyse the data for a few more kilometers of altitude coverage.

Figure 6, which plots the mean hourly event rate as function of the estimated target diameter, gives an indication of the effective detection sensitivity in the QS. The smallest included targets are about 3.5 cm in the 700-1000 km zone (zone 2), and about 5.0 cm in the 1300-1600 km zone (zone 3). In both these zones, it is apparent from Fig. 6a that the small-size end of the distribution is affected by the strong post-detection event filtering. The distribution must be similarly affected also in the lowest zone, but there the greater relative variation of range within the zone better masks the sharp cutoff. The size distributions vary slightly from day to day. For example, around the ASAT altitude of 860 km the daily median value of the diameter distribution varies in a random-looking manner throughout the IPY, with mean value of 5.8 cm and a standard deviation of 0.4 cm. The median values might be slightly higher during the summer time than during the winter time, though, see Fig. 6b. Were this indeed so, the reduced sensitivity could be due to the increased ionospheric clutter during the summer.

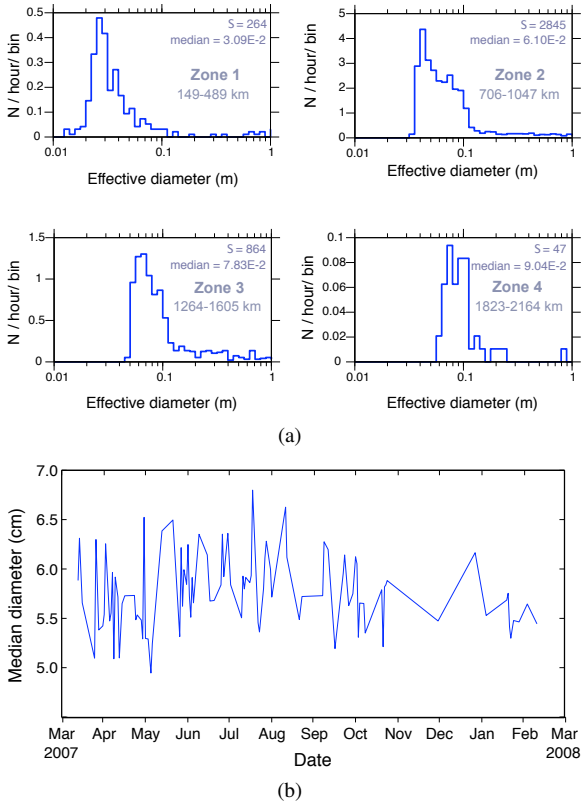

Figure 6. (a) Mean hourly event rate as function of effective diameter in the four IPY altitude zones. Four dates between 23 Jul and 28 Jul 2007 were used for the hourly averaging. (b) Median daily value of the effective diameter in a 50 km wide zone centered at 860 km altitude. There may be a slight seasonal variation in the median data.

Inspection of daily time-altitude-Doppler plots in the QS, such as Fig. 5, reveals considerable differences in the shape of the ASAT-related cluster of observation points in different times of the year: sometimes the cluster is concentrated near the original fragmentation altitude, while in other times it is more evenly spread. The left-hand panels of Fig. 9 show this apparent "pulsation" of the ASAT cloud quite clearly. However, the daily event count in Fig. 1, which contains all the data from all altitude zones, does not show any drastic differences from day to day. The pulsation only comes apparent when one limits the event count to a rather narrow zone around the fragmentation altitude. This we have done in Fig. 7, where we have plotted the daily event count in three 20 km wide zones centered at altitudes 830 km, 860 km, and 900 km. In the 860 km zone, there is a clear increase, by about 150%, in the event count over a "background" level, with a period of about four months. A roughly similar variation extends about 30 km on both sides of the 860 km altitude, but then rapidly disappears.

Eccentricity oscillations with a period of about 120 days, though with smaller magnitude, had been observed at fragments from Ariane V 16 explosion in 1986 at 800 km

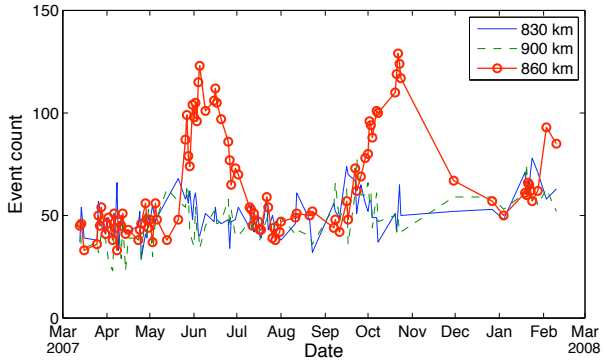

Figure 7. "Pulsation" of daily event count. Plotted is the daily event count in three 20 km wide altitude zones for all days of the Quality Set. There is strong variation, with a period of about four months, but only in the zone around the original ASAT fragmentation altitude of 860 km.

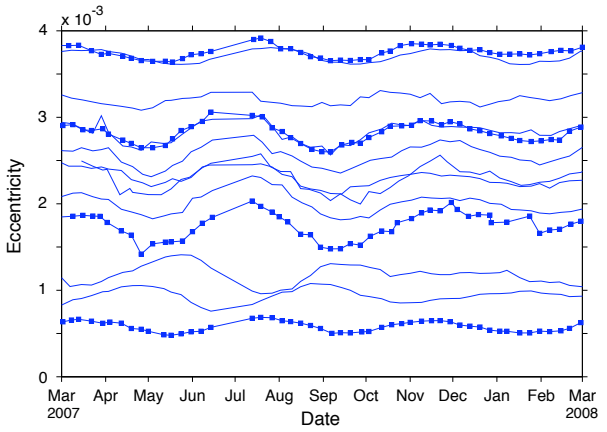

Figure 8. Orbit eccentricity of a few ASAT (1999-25A) fragments during the IPY, according to ESA DISCOS database.

altitude on a 98° inclination orbit, a situation similar to the ASAT case [8]. The oscillations were then explained with the perturbation caused by the J_3 term of the Earth's gravity field. As Fig. 8 shows, such eccentricity oscillations are present also in the ASAT cloud. However, they cause variations in orbit altitude only on the order of 10-15 km, and are too small to explain the observed variation in the event count.

Simulation of the ASAT cloud with the ESA PROOF tool (Fig. 9) showed that the only orbital parameter of the fragments that changes significantly over time is the argument of perigee (AOP). The change is due to perturbations induced by the oblateness term J_2 of the Earth's gravity field. The apparent pulsation is due to the precession of the "pinch point" (e.g. [9], p. 73) of the ASAT cloud along the orbital plane. The AOP drift causes all orbits to rotate, hence also the pinch point is rotating. When the pinch point comes above the radar site, one gets high event count in the original fragmentation altitude, while 90° away from the pinch point, the orbits are maximally spread in altitude.

Figure 9 shows that the simulation is able to reproduce the observed event clustering and spreading qualitatively rather well. Except for the early phase of the campaign, also the observed and simulated peak event densities are compatible. However, on 13 March 2007 the observed maximum event count is nearly a factor of two lower than predicted. It is possible that the discrepancy can be explained by the fact that the EISCAT detection algorithm could not cope with too many almost-simultaneous events.

—

EISCAT is an international association supported by research organisations in China (CRIRP), Finland (SA), France (CNRS, till end 2006), Germany (DFG), Japan (NIPR and STEL), Norway (NFR), Sweden (VR), and the United Kingdom (STFC).

REFERENCES

[1] Markkanen J., Lehtinen M., Huuskonen A., Väänänen, A., (2002). Measurements of Small-Size Debris with Backscatter of Radio Waves, Final Report, ESOC Contract No. 13945/99/D/CD. On-line as `www.sgo.fi/~jussi/spade/FR_16Apr2002.pdf`

[2] Markkanen J., Postila M., (2005). Real-Time Small-Size Space Debris Detection with EISCAT Radar Facilities, Final Report, ESOC Contract No. 16646/02/D/HK(CS). On-line as `www.sgo.fi/~jussi/spade/FRII_21feb2005.pdf`

[3] Markkanen J., Lehtinen M., Landgraf M., (2005). Real-time space debris monitoring with EISCAT, Advances in Space Research 35, 1197-1208

[4] Markkanen J., Postila M., van Eyken A., (2005). Small-Size Space Debris Data Collection with EISCAT Radar Facilities, Final Report, ESOC Contract No. 18575/04/D/HK(SC). On-line as `www.sgo.fi/~jussi/spade/FRIII_26july2006.pdf`

[5] Krag H., Klinkrad H., Jehn R., Markkanen J., Leushacke L., (2007). Detection of Small-Size Space Debris with the FGAN and EISCAT Radars, Proc. 7th US-Russian Space Surveillance Workshop

[6] Jehn R., Klinkrad H., Krag H., Flohrer T., Leushacke L., Markkanen J., Schildknecht T., Oswald M., (2008). Space Traffic Data Analysis and Synthesis, 3rd International Association for the Advancement of Space Safety Conference, Rome, Italy, 21-23 October 2008

[7] Vierinen J., Markkanen J., Lehtinen M., (2009). Measuring Space Debris with Phase Coded Aperiodic Transmission Sequences, In these Proceedings

[8] Jehn R., (1996). Modelling Debris Clouds, Doctoral Theses

[9] Klinkrad H., (2006). Spade Debris, Models and Risk Analysis, Praxis Publishing Ltd

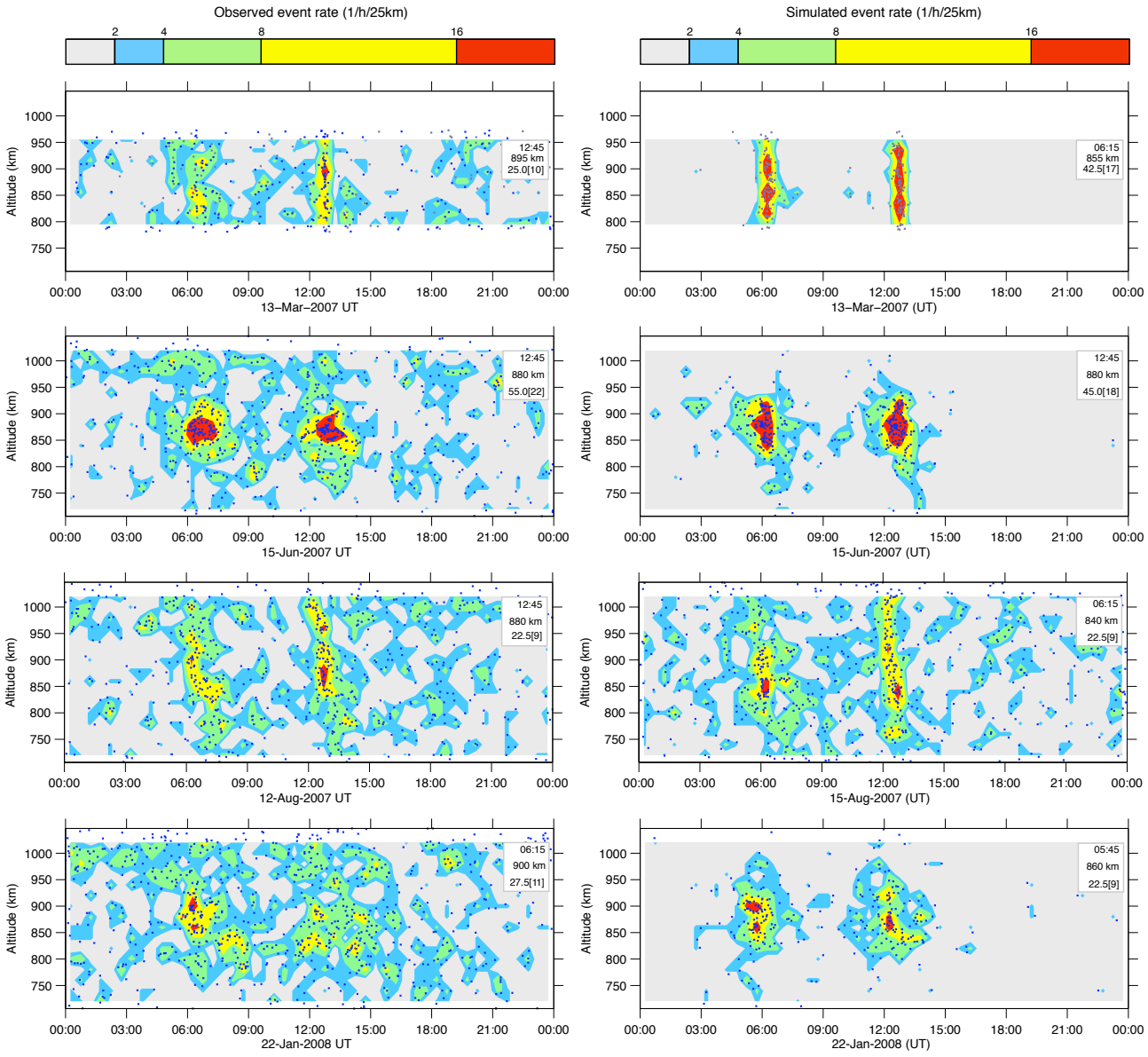

Figure 9. Time development of the Chinese ASAT cloud during the IPY as observed by EISCAT. The left-hand-side panels are the EISCAT observations for four days in the Quality Set, the right-hand-side panels are simulated observations, computed with the ESA PROOF tool for the same (or nearly same) dates. In the simulation plots, only the ASAT fragments are plotted, except for 15 Aug, where also the background debris has been generated. The time-altitude dots are the daily observations and the simulated observations, respectively. The colour contours display the event density, using a rough, logarithmic scale. The insert in the top-right corner of each panel gives the time, altitude, and value of the peak event density of the day.